Excitation cross sections in low-energy hydrogen-helium collisions

Andrey K. Belyaev*
Department of Theoretical Physics, Herzen University, St. Petersburg 191186, Russia
(Received 13 May 2015; published 23 June 2015)

Quantum chemical results for the lowest four potentials of the HeH molecule and the corresponding rotational and radial nonadiabatic coupling matrix elements are reported. Close-coupling calculations of the integral cross sections for the excitation processes $H(1s) + He \rightarrow H(2s,2p) + He$ are performed on this basis. The calculated cross sections are in a reasonable agreement with the experimental data.

DOI: 10.1103/PhysRevA.91.062709 PACS number(s): 34.10.+x, 34.50.Fa, 95.30.Dr

I. INTRODUCTION

Inelastic processes determine properties of gaseous and plasma media in many cases, in particular, for nonlocal thermodynamic equilibrium effects which are important in astrophysics and plasma physics, especially when hydrogen and/or helium are involved [1]. Inelastic collision processes are of particular importance. The main source for inelastic collision process data is numerical calculations. A vast majority of these calculations are performed within the Born-Oppenheimer (BO) approach, which treats a collision in terms of molecular states. The calculation of inelastic atom-atom collision cross sections forms a straightforward application of numerical quantum mechanics. Within the BO formalism, the potential energy curves, the radial and rotational coupling matrix elements of the collision pair are required as input data for a close-coupling procedure yielding the collisional channel wave functions, the nonadiabatic transition probabilities, and the cross sections. Using the molecular-state representation (and molecular coordinates) within the BO formalism leads to the so-called molecular-state (or electron-translation) problem, which formed a severe problem for many years; see, e.g., [2–6]. The problem can now be solved by different methods beyond the BO approach [3,7–9], as well as within the BO formalism [4–6]. In the present study, the molecular-state problem for inelastic H + He collisions is resolved by means of the reprojection method [4–6] within the BO approach. The reprojection method does not require calculations of any additional quantum chemical values; it is based on only fixed-nuclear potentials and nonadiabatic couplings computed with the electronic coordinate origin at the center of nuclear mass.

The HeH system with only three electrons offers itself as a testing ground for our theoretical capabilities in this field. Calculations of the adiabatic potential energy curves leading to the ground and low-lying excited states of the HeH molecule and of the corresponding coupling matrix elements are reported and discussed in the present paper. The integral cross sections for the processes

$$H(1s) + He \rightarrow H(2s,2p) + He \qquad (1)$$

obtained on this basis are computed and found to be in a reasonable qualitative agreement with available experimental data.

*andrey.k.belyaev@gmail.com

II. QUANTUM CHEMICAL CALCULATIONS

The quantum chemical calculations [5] were carried out on the configuration-interaction level, using a code developed by Hirsch *et al.* [10] and Bruna and Peyerimhoff [11] [the multireference single- and double-excitation configuration-interaction (MRD-CI) method] and a basis of $17s$, $10p$, and $2d$ atomic orbitals, each centered at one of the two atoms. The electronic states $X\,^2\Sigma^+$, $A\,^2\Sigma^+$, $B\,^2\Pi$, and $C\,^2\Sigma^+$, which converge to the ground and first excited levels of the pair of separated atoms, are considered here.

Figure 1(a) shows the adiabatic potential curves $U_{j\Lambda}(R)$, R being the internuclear distance; logarithmic scales are used in order to bring out the repulsive branch more clearly. Figure 1(b) shows the differences between the potentials of the excited states and that of the ground state. The calculations were carried out down to distances of 0.05 a.u., where the system is close to the united atom limit. The experimental energy level differences of the united atom Li are shown as black squares. The good agreement emphasizes the good quality of the present results even in the strongly repulsive short range. Similarly, the excitation energy for the free H atom at $R \rightarrow \infty$ was always found to come out at the expected value of 0.375 a.u. within narrow limits.

The radial coupling matrix elements are the quantities $\langle j\ \Lambda|\partial/\partial R|k\ \Lambda\rangle$ and the rotational coupling elements are $\langle j\ \Lambda|iL_y|k\ \Lambda \pm 1\rangle$, where $|j\ \Lambda\rangle$ are the electronic molecular wave functions and L_y is the component of the electronic orbital angular momentum operator perpendicular to the internuclear axis. The calculated values of the matrix elements are shown in Figs. 2(a) and 2(b), respectively. The operation $\partial/\partial R$ is a partial derivative; it was carried out with the electron coordinates fixed with respect to the center of mass of the two nuclei in order to reach the simplest and standard form of the nuclear dynamical equations [4,12]. Similarly, L_y was computed with respect to the center of nuclear mass. Figure 2(a) is dominated by a peak at 0.8 a.u. in the XA curve, which reflects an avoided crossing between the $X\,^2\Sigma^+$ and $A\,^2\Sigma^+$ states. The corresponding minimum in the XA potential difference is clearly visible in Fig. 1(b). The molecular X and A states interchange their character in the crossing region, which is witnessed by the rapid variation of the rotational coupling elements in the figure in this area.

The important feature of the quantum chemical calculation is nonvanishing values of the radial couplings in the asymptotic ($R \rightarrow \infty$) region:

$$\langle X\,^2\Sigma|\partial/\partial R|A\,^2\Sigma\rangle_\infty = -0.1299 \text{ a.u.}, \qquad (2)$$

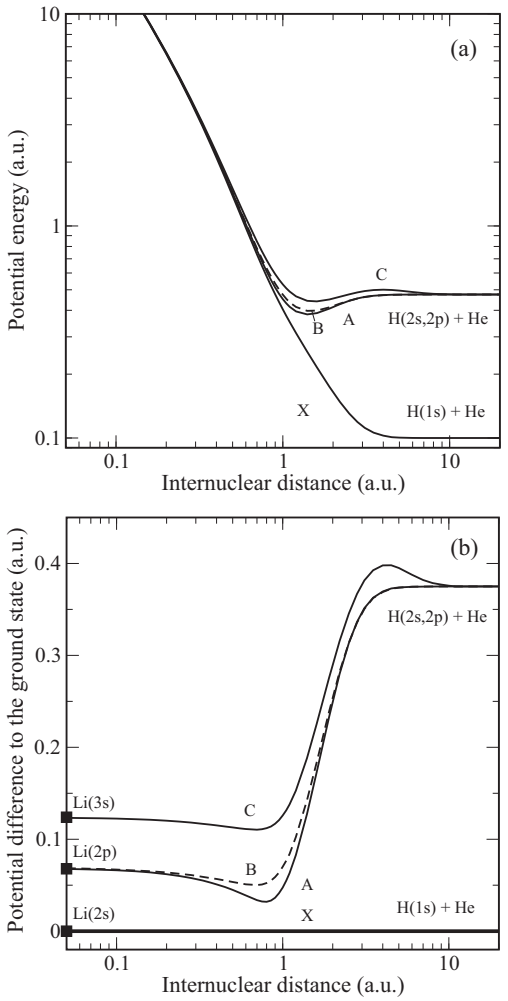

FIG. 1. The $X\,^2\Sigma^+$, $A\,^2\Sigma^+$, $C\,^2\Sigma^+$, and $B\,^2\Pi$ adiabatic potential energy curves of HeH (a), and the differences of the potentials from the ground-state potential, with the ground-state potential set to zero (b). The molecular states are identified by the first letter.

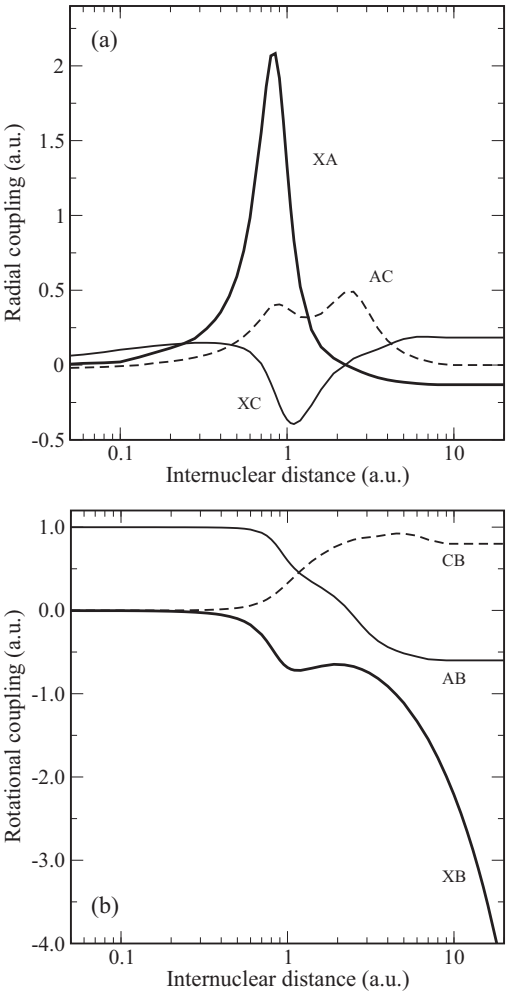

FIG. 2. The radial (a) and rotational (b) coupling matrix elements. The adiabatic molecular states $X\,^2\Sigma^+$, $A\,^2\Sigma^+$, $C\,^2\Sigma^+$, and $B\,^2\Pi$ are identified by the first letter.

$$\langle X\,^2\Sigma|\partial/\partial R|C\,^2\Sigma\rangle_\infty = 0.1819 \text{ a.u.}; \tag{3}$$

see Fig. 2(a). Nonzero asymptotic radial couplings are a fundamental feature of the standard BO approach. Indeed, the asymptotic radial couplings calculated with the electron origin at the center of nuclear mass read

$$\langle j\Lambda|\frac{\partial}{\partial R}|k\Lambda\rangle_\infty = \gamma\,\frac{m}{\hbar^2}[U_{j\Lambda}(\infty) - U_{k\Lambda}(\infty)]\langle j\Lambda|d_z|k\Lambda\rangle, \tag{4}$$

where γ is the scalar factor, at present $\gamma = M_{\rm He}/(M_{\rm He} + M_{\rm H})$, m the electron-nuclei reduced mass, and $\langle j\Lambda|d_z|k\Lambda\rangle$ the electronic transition dipole moment calculated on asymptotic molecular wave functions; see [4–6,12] for details. Usually, asymptotic molecular wave functions converge into (products of) atomic wave functions, and, therefore, $\langle j\Lambda|d_z|k\Lambda\rangle$ are expected to be equal to the atomic transition dipole moments. However, in the present case of H + He collisions, the excited states are asymptotically degenerate and the asymptotic molecular states are linear combinations of (products of) atomic states: $|j\ \Lambda\rangle = \underline{B}\ |{\rm H}(nl\lambda) + {\rm He}\rangle$ ($\lambda = \sigma,\pi,\ldots$), that is,

$$\begin{pmatrix} |X\,^2\Sigma\rangle \\ |A\,^2\Sigma\rangle \\ |C\,^2\Sigma\rangle \\ |B\,^2\Pi\rangle \end{pmatrix} = \underline{B} \begin{pmatrix} |{\rm H}(1s\sigma) + {\rm He}\rangle \\ |{\rm H}(2s\sigma) + {\rm He}\rangle \\ |{\rm H}(2p\sigma) + {\rm He}\rangle \\ |{\rm H}(2p\pi) + {\rm He}\rangle \end{pmatrix}, \tag{5}$$

where

$$\underline{B} = \begin{pmatrix} 1 & 0 & 0 & 0 \\ 0 & \alpha & \beta & 0 \\ 0 & -\beta & \alpha & 0 \\ 0 & 0 & 0 & 1 \end{pmatrix} \tag{6}$$

is a composition unitary matrix, and α and β are some coefficients satisfying the condition $|\alpha|^2 + |\beta|^2 = 1$. In this case, the asymptotic radial couplings are equal to linear combinations of derivative matrix elements calculated on atomic wave functions. Taking into account that $\langle 1s\sigma|\partial/\partial R|2s\sigma\rangle = 0$, one has in the asymptotic region

$$\langle X\,^2\Sigma|\frac{\partial}{\partial R}|A\,^2\Sigma\rangle_\infty = \beta\ \langle 1s\sigma|\frac{\partial}{\partial R}|2p\sigma\rangle, \tag{7}$$

$$\langle X\,^2\Sigma|\frac{\partial}{\partial R}|C\,^2\Sigma\rangle_\infty = \alpha\,\langle 1s\sigma|\frac{\partial}{\partial R}|2p\sigma\rangle. \quad (8)$$

Equations (7) and (8) explain why there are two nonvanishing asymptotic radial couplings, *XA* and *XC*, in the quantum chemical calculations although there is only one nonzero atomic transition dipole moment between the states treated. The matrix element $\langle 1s\sigma|\partial/\partial R|2p\sigma\rangle$ can be calculated analytically; it has the value 0.2235 a.u. Taking the matrix elements $\langle X\,^2\Sigma|\partial/\partial R|A\,^2\Sigma\rangle_\infty$ and $\langle X\,^2\Sigma|\partial/\partial R|C\,^2\Sigma\rangle_\infty$ from the quantum chemical calculations Eqs. (2) and (3), one gets $\alpha = 0.8138$ and $\beta = -0.5812$; see Eqs. (7) and (8). These coefficients determine the composition matrix $\underline{B}$; see Eq. (6).

Another important feature of the quantum chemical results is an infinite increase of the absolute value of the asymptotic *XB* rotational coupling; see Fig. 2(b). Again, this is a fundamental characteristic of using the molecular representation within the standard BO approach; see Eq. (20) in Ref. [5]. Indeed, the nonvanishing limits of the radial couplings reflect a mere electron translation effect: the electron wave functions move with one of the nuclei when the distance R becomes large and not with the center of nuclear mass, which was used as the origin when calculating the matrix elements. The increase of the *XB* term towards large R in Fig. 2(b) has a similar origin. The large-R limits of radial as well as rotational matrix elements can be changed by choosing another origin, but this would lead to additional terms in both the total Hamiltonian and the coupled-channel equations. These additional terms would compensate changing of the couplings and keep the same nonzero terms in the dynamical equations; see [4,12]. A similar conclusion has been made in Refs. [13,14]. Thus, special care should be taken in nonadiabatic nuclear dynamics about both features concerning the radial and rotational asymptotic couplings.

III. NONADIABATIC NUCLEAR DYNAMICS

The quantum mechanical scattering problem can be cast into the form of a system of coupled equations, where the coupling terms between different $^2\Sigma^+$ states are proportional to the radial coupling elements and those between $^2\Sigma^+$ and $^2\Pi$ states to the rotational coupling elements divided by R^2. The coupled equations contain not only first- but also second-order derivative coupling terms. The rotational coupling terms of this type were neglected; the corresponding radial coupling terms, which are required for the conservation of current, were modeled by first-order terms as described in Ref. [15]. Owing to the finite number of electronic states considered, the coupled system is truncated to four coupled equations in the present treatment. The nonzero asymptotic *XA* and *XC* radial couplings discussed above imply inelastic transitions between electronic molecular states at arbitrarily large distance, but inelastic transition probabilities should be calculated not between molecular states, they should be computed between electronic scattering states in the asymptotic region, and the reprojection method takes this into account. The reprojection method consists in solving the coupled equations with the matrix elements as they are shown, and taking corresponding care when constructing the correct asymptotic scattering wave functions from the numerical solution. The important point is that each single incoming and outgoing asymptotic wave function for a scattering (atomic) channel written in scattering coordinates in the asymptotic region populates several molecular wave functions written in molecular coordinates at a projection distance, and vice versa. The form of the coupled equations and the way in which the S matrix is obtained from the channel wave functions are discussed in detail in Ref. [5]. The reprojection method is generalized in Ref. [6] for multielectron collision systems.

The neglect of the molecular-state problem, that is, treating an inelastic probability as a transition probability between molecular states instead of a transition probability between scattering (atomic) states (which is in turn a result of the neglect of the difference between internuclear and interatomic coordinates in asymptotic wave functions) leads to a severe problem, which is twofold. (i) The inelastic transition probability calculated as a probability between molecular states in the asymptotic region remains an oscillatory function of the upper integration limit [4–6]. This oscillatory behavior results in some uncertainty for the inelastic transition probability. This uncertainty might be small as compared to a rigorous transition probability, but if the rigorous probability has a small value, the uncertainty might be much larger than the probability itself; see [6]. (ii) Since nonadiabatic transitions between molecular states remain at arbitrarily large internuclear distance, then nonadiabatic transition probabilities remain nonzero at arbitrarily large total angular momentum quantum number J. This leads to a lack of convergence of the inelastic cross section with respect to the summation over J which goes to ∞ [6]; so the calculated inelastic cross section might have no sense. The reprojection method [4–6] resolves both problems.

Degeneracy of the excited hydrogen states observed in the present study adds an extra complication. In order to calculate the final scattering matrix $\underline{S}^{\text{final}}$ from the scattering matrix $\underline{S}$ computed from the coupled equations by means of the reprojection method [5], one has to apply the additional transformation with the composition matrix $\underline{B}$ defined by Eq. (6):

$$\underline{S}^{\text{final}} = \underline{B}^\dagger\,\underline{S}\,\underline{B}. \quad (9)$$

The inelastic cross sections are calculated from the $\underline{S}^{\text{final}}$ matrix as usual.

Figure 3 shows the calculated inelastic cross sections for collision energies from the threshold to 1 keV. The light lines are the integral cross sections for H($2p\sigma$) and H($2p\pi$) production, which add up to the H($2p$) cross section shown by the upper heavy line. The lower heavy line is the integral cross section for H($2s$) production. At the lowest energies, H($2p\sigma$) formation dominates, indicating that radial coupling is the only relevant mechanism here. We deal at low energy essentially with the $X \to A$ transition induced by the avoided crossing at 0.8 a.u. With increasing energy, H($2p\pi$) production soon becomes comparable, indicating the growing importance of rotational coupling. Rotational coupling between the converging X and B states near the united atom limit is a very effective mechanism, which is however suppressed at the lowest energies because the necessary close approach of the nuclei is not possible. Figure 1(a) shows how small distances become more and more accessible with increasing energy, leading to an increasing weight of the rotational coupling mechanism. The asymptotic population of the B state is completely found back as the atomic $2p$

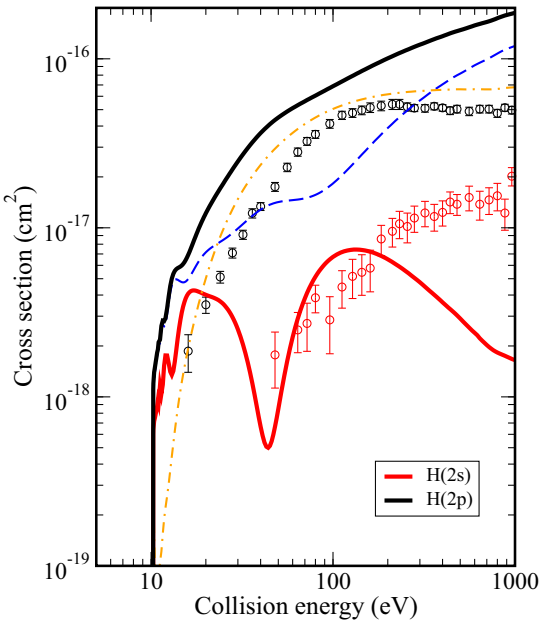

FIG. 3. (Color online) The cross sections as functions of the relative energy. Heavy lines: numerical results for H($2s$) (lower, red line) and H($2p$) (upper, black line). Light lines: the partial cross section for H($2p\sigma$) (blue dashed line) and H($2p\pi$) (orange dot-dashed line). Symbols: H($2p$) production (upper, black) and an upper limit for H($2s$) production (lower, red).

population. Rather, the population of the A and C molecular states is redistributed into H($2s$) and H($2p$) populations, according to the asymptotic composition (5) of the molecular states. The small value of the $2s$ cross section compared to $2p\sigma$ is therefore an interference effect, reflecting a comparable asymptotic population of the A and C states and a relative phase favoring superposition to form $2p$.

The symbols in Fig. 3 are experimental results [16]. They were derived from measurements of the Ly-α emission, the increase of the emission under the influence of an electric field. The data had to be corrected for cascades. Due to the related uncertainty, the $2s$ data form only an upper limit to the actual $2s$ production cross section. Experimental and theoretical data agree with respect to the order of magnitude of the cross sections, with respect to the relative magnitude of the $2s$ and $2p$ cross sections, and with respect to the comparatively slow increase of the cross sections with the energy. However, discrepancies of up to a factor of 3 remain between experiment and theory. In previous similar applications to more complex collisional systems (see, e.g., Na + H [15]) the typical remaining discrepancy was not larger than a factor of 2. For the present simple system, a better agreement might have been expected.

IV. CONCLUSION

Possible sources of deviation between the experimental and numerical data can have various origins: (i) A major shortcoming of the experimental data consists in the highly indirect procedure used for determining the absolute cross section scale. The data were normalized for this purpose to results published by other authors, which in turn relied again on a similar normalization. The error of the experimental data in Fig. 3 was estimated to be of the order of 40% [16]. A larger error of the absolute scale seems possible, however, and offers a straightforward explanation for a large part of the observed discrepancy. (ii) The neglect of higher excited states in the system of coupled equations. Inclusion of the molecular states leading to H($n = 3$) can therefore be expected to have some effect on the numerical results, but would probably not lead to changes beyond a few tens of percent. Generally, one expects errors of this type to be less relevant for the range of energies near the threshold, compared to the 1 keV range. (iii) Errors in the calculated potentials and coupling matrix elements are expected to be smaller than for the Na + H system referred to above and should therefore in general result in correspondingly smaller deviations.

In summary, the numerical treatment of the present system offers no severe conceptual or mathematical difficulties, either on the quantum chemical or on the dynamical level. The degree of agreement with the experimental data makes a repetition of the experiment highly desirable.

ACKNOWLEDGMENTS

The author gratefully acknowledges Professor J. Grosser for fruitful discussions and the Ministry for Education and Science (Russian Federation) for support of the work.

[1] M. Asplund, Annu. Rev. Astron. Astrophys. **43**, 481 (2005).
[2] D. R. Bates and R. McCarroll, Proc. R. Soc. London, Ser. A **245**, 175 (1958).
[3] J. B. Delos, Rev. Mod. Phys. **53**, 287 (1981).
[4] J. Grosser, T. Menzel, and A. K. Belyaev, Phys. Rev. A **59**, 1309 (1999).
[5] A. K. Belyaev, D. Egorova, J. Grosser, and T. Menzel, Phys. Rev. A **64**, 052701 (2001).
[6] A. K. Belyaev, Phys. Rev. A **82**, 060701(R) (2010).
[7] L. F. Errea, L. Méndez, and A. Riera, J. Phys. B: At. Mol. Phys. **15**, 101 (1982).
[8] C. D. Lin, Phys. Rep. **257**, 1 (1995).
[9] D. Rabli and R. McCarroll, J. Phys. B: At. Mol. Opt. Phys. **38**, 3311 (2005).
[10] G. Hirsch, P. J. Bruna, R. J. Buenker, and S. D. Peyerimhoff, Chem. Phys. **45**, 335 (1980).
[11] P. J. Bruna and S. Peyerimhoff, Adv. Chem. Phys. **67**, 1 (1987).
[12] A. K. Belyaev, A. Dalgarno, and R. McCarroll, J. Chem. Phys. **116**, 5395 (2002).
[13] B. Zygelman, D. L. Cooper, M. J. Ford, A. Dalgarno, J. Gerratt, and M. Raimondi, Phys. Rev. A **46**, 3846 (1992).
[14] G. J. Bottrell, Nucl. Instrum. Methods Phys. Res., Sect. B **79**, 173 (1993).
[15] A. K. Belyaev, J. Grosser, J. Hahne, and T. Menzel, Phys. Rev. A **60**, 2151 (1999).
[16] J. Grosser and W. Krüger, Z. Phys. A **318**, 25 (1984).